Supplemental Data

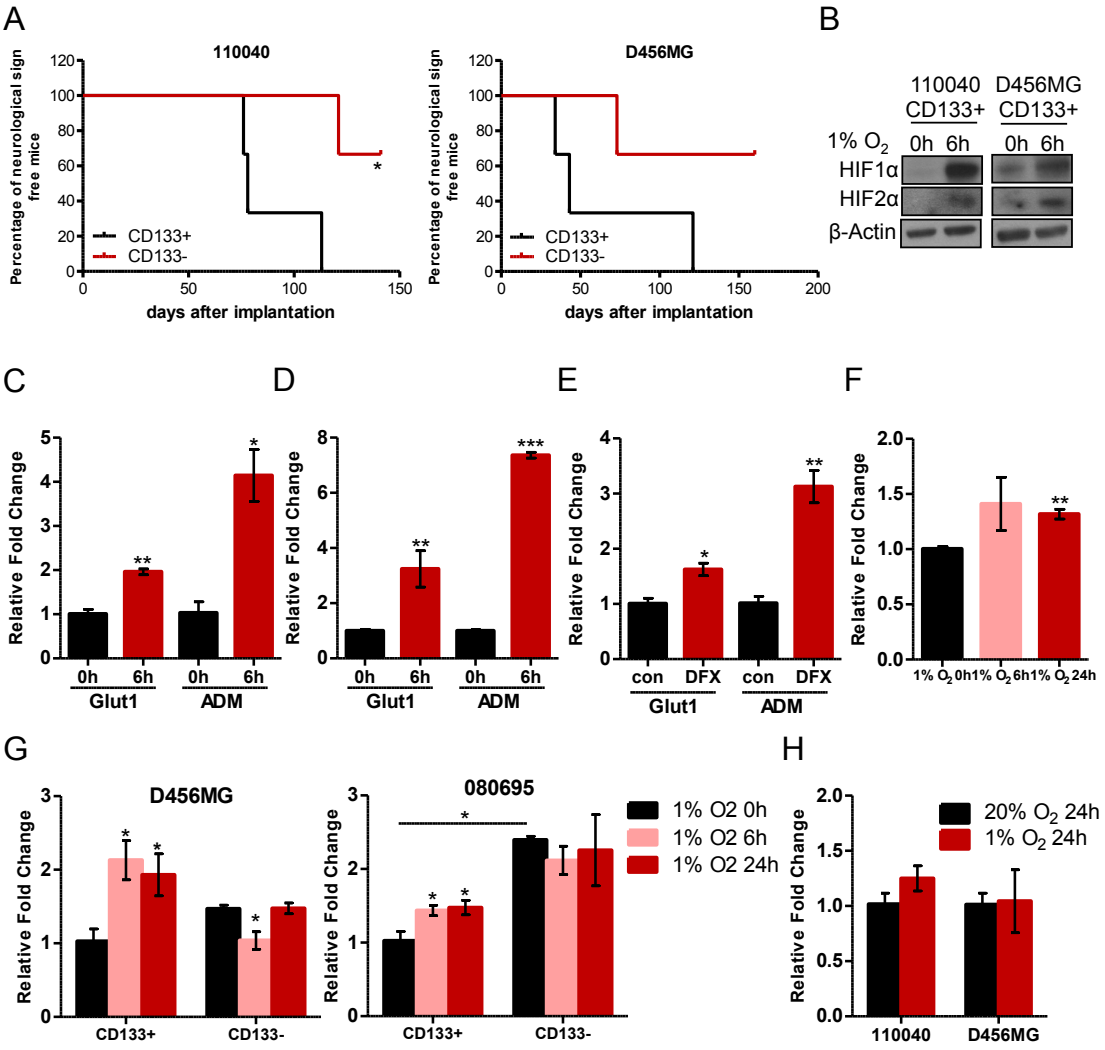

Figure S1, Related to Figure 1. MiR-215 is induced in GICs cultured under hypoxia. (A) Kaplan-Meier curves were drawn to measure the burden of tumor progression by $CD133^+$ or $CD133^-$ cells isolated from D456MG and 110040. 1000 $CD133^+$ or $CD133^-$ cells were injected intracraniallly for D456MG and 110040. n=3.(B) Protein level of HIF1α and HIF2α were measured in $CD133^+$ GICs isolated from 110040 and D456MG. β-Actin was used as an internal control. (C, D) Expression changes of the hypoxia-responsive genes Glut1 and ADM were determined by qPCR in GICs isolated from 110040 (C) and D456MG (D) when cultured in 1% O_2 for 6 hrs. n=3. (E) Expression changes of Glut1 and ADM were shown in GICs isolated from D456MG and treated with 10μM DFX for 3 hrs. n=3. (F) Expression of miR-215 was shown in $CD15^+$ GICs isolated from D456MG when cultured in 1% O_2 for 6 hrs and 24 hrs. n=3. (G) Expression of miR-215 was shown in matched $CD133^+$ GICs and $CD133^-$ non-GICs isolated from D456MG and 080695 when cultured in 1% O_2 for 6 hrs and 24 hrs. n=3. (H) Expression of miR-194 was not changed in GICs cultured in hypoxia from the same experiment as Figure 1D. n=4. ACTB was used as an internal control for the measurement of Glut1 and ADM; RNU6 was used as an internal control for mature miR-215 and miR-194. Data are represented as the mean ± SEM. (* $p<0.05$, ** $p<0.01$)

Table S1, Related to Figure 1. MiRNA expression profiles from the miRNA qPCR array

A separate excel file of the miRNA qPCR array is attached. Fold changes and p values of 85 miRNAs from GICs cultured in hypoxia compared to those cultured under normoxia in two different xenografted glioma lines (11-0040, D456MG) are listed.

Table S2, Related to Figure 1. MiRNAs induced consistently by hypoxia

$CD133^+$ GICs isolated from two different glioma xenografted lines 110040 and D456MG were cultured under hypoxia (1% O_2 or DFX treatment) for the indicated times, followed by the miRNA qPCR array. 11 miRNAs were deregulated consistently (Threshold: fold change more than 1.2 in each group and p value less than 0.1). Two-tailed paired t test was used for statistical analysis.

miRNA ID	11-0040 1% O_2 6h	D456MG 1% O_2 6h	D456MG DFX 3h	p value
hsa-miR-215	1.82	2.19	2.64	0.02
hsa-miR-218	2.18	3.46	4.31	0.03
hsa-miR-518b	2.12	2.19	3.60	0.03
hsa-miR-520g	1.75	1.63	2.57	0.04
hsa-miR-134	1.43	2.43	2.42	0.06
hsa-miR-129-5p	2.32	2.16	5.57	0.07
hsa-miR-127-5p	1.65	1.79	3.24	0.07
hsa-miR-122	1.54	1.79	3.19	0.08
hsa-miR-96	1.68	1.22	1.28	0.08
hsa-miR-370	2.06	1.31	2.61	0.08
hsa-miR-155	1.21	2.19	1.96	0.09

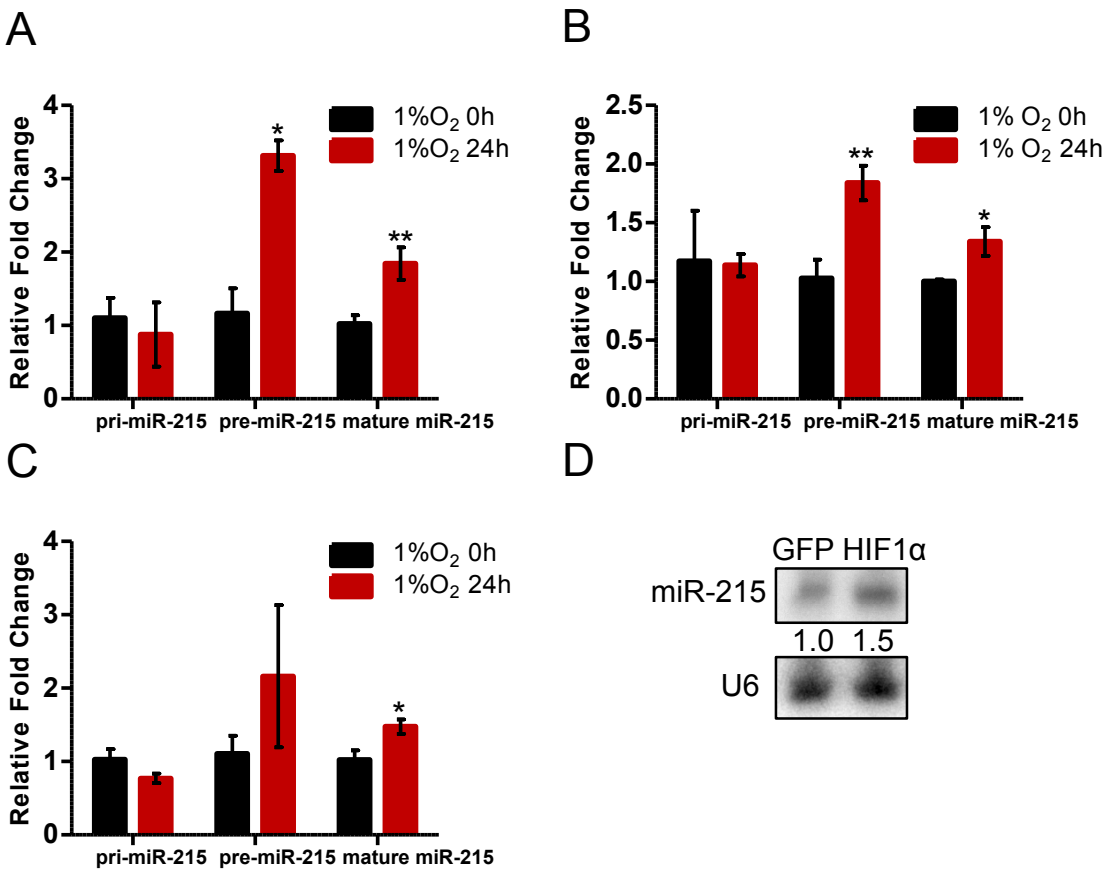

Figure S2, Related to Figure 2. Biogenesis of pri-miR-215 to pre-miR-215 is enhanced through HIF. (A-C) Expression profiles of pri-, pre- and mature miR-215 were examined by qPCR in GICs isolated from D456MG (A), GSC20 (B) and 080695 (C) cultured in 1% O_2 for 24 hrs. n=4. (D) Expression level of mature miR-215 was detected by northern blot in HEK293T cells transfected with pri-miR-215 and a stabilized HIF1α or GFP control. Same RNAs were used from Figure 2D. U6 was used as an internal control for northern. ACTB was used as an internal control for the measurement of pri-miRNAs; RNU6 was used as an internal control for pre- and mature miRNAs. Data are represented as the mean ± SEM. (* $p<0.05$, ** $p<0.01$)

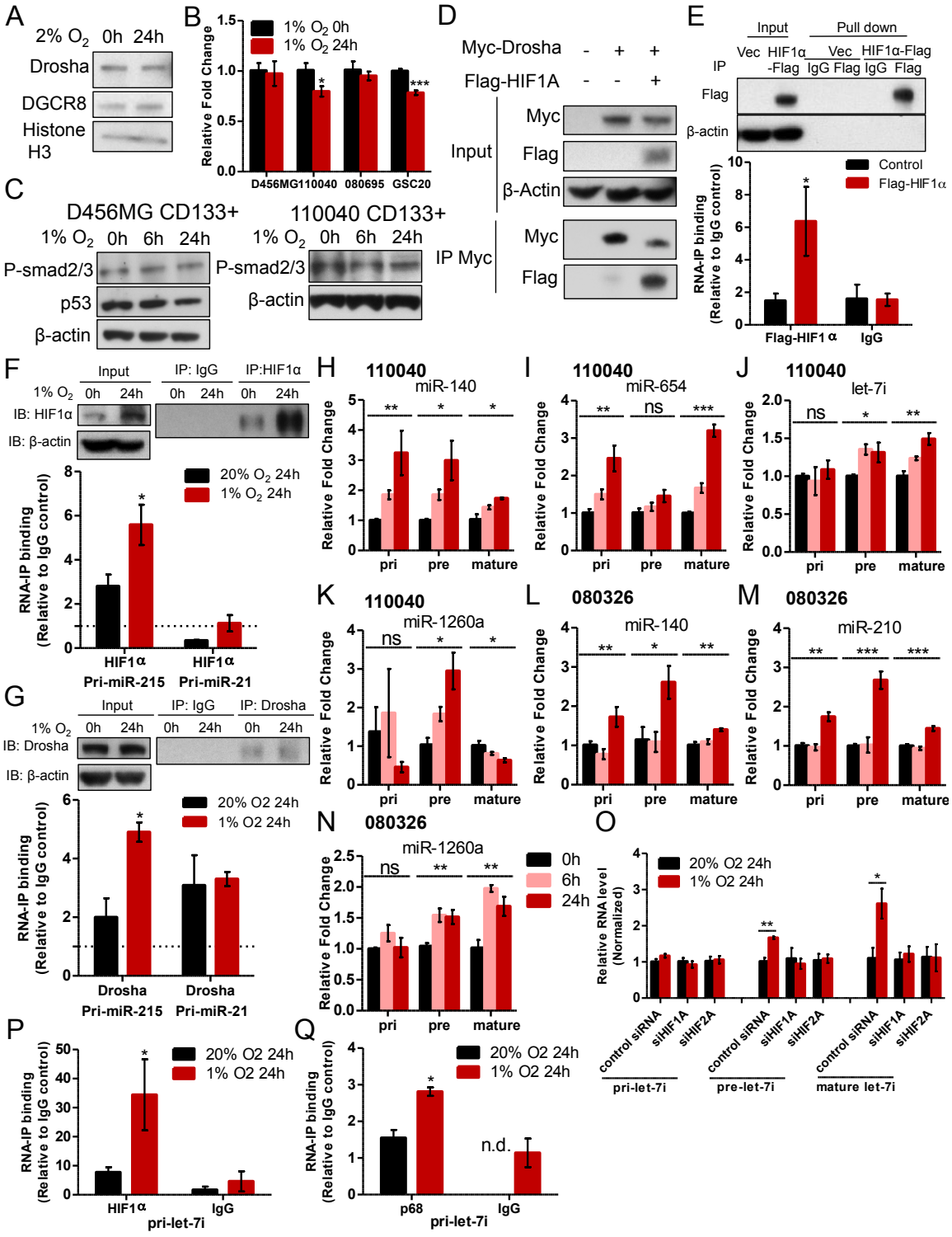

Figure S3, Related to Figure 3. HIF1α interacts with Drosha/DGCR8 complexes and enhances incorporation of pri-miRNAs into the complex to promote processing. (A) Immunoblots were performed to detect protein levels of Drosha and DGCR8 in 110040 GICs cultured under 2% O_2 or 20% O_2.

(B) Expression level of Dicer was measured by qPCR in GICs isolated from D456MG, 110040, 080695 and GSC20 cultured under 1% O_2 for 24 hrs. n=4. (C) Immunoblots were performed to detect levels of P-smad2/3 and p53 in GICs isolated from D456MG and 110040 when cultured under 1% O_2 for the indicated time points. No p53 was detected in 110040 GICs. (D) Myc-tagged Drosha and Flag-tagged HIF1α was transfected separately or in combination into HEK293T cells followed by immunoprecipitation with the Myc antibody. (E) RNA-ChIP was used to detect the association between HIF1α and pri-miR-215 when a stabilized Flag-tagged HIF1α mutant was transfected into HEK293T cells over-expressing pri-miR-215. HIF1α was immunoprecipitated using the Flag antibody, as shown by Western blot in the upper panel. Incorporation of pri-miR-215 into the HIF1α complex was examined by qPCR as displayed in the lower panel. IgG was used as a negative control. n=4. (F-G) HIF1α (F) or Drosha (G) was immunoprecipitated using lysates from D456MG $CD133^+$ GICs, as shown by Western blot in the upper panels. Incorporation of pri-miR-215 or pri-miR-21 into the protein complex was examined by qPCR as displayed in the lower panels. IgG was used as a negative control and dotted lines indicate the background level of non-specific binding of pri-miRNAs to IgG.. n=4. (H-K) Expression profiles of the pri-, pre- and mature forms of miR-140 (H), miR-654 (I), let-7i (J) and miR-1260a (K) were examined in GICs isolated from 110040 by qPCR. n=3. (L-N) Expression pattern of the pri-, pre- and mature forms of miR-140 (L), miR-210 (M) and miR-1260a (N) was determined in GICs isolated from the glioma xenografted line 080326 by qPCR. n=3. (O) Expression pattern of pri-, pre- and mature let-7i was examined by qPCR in GICs isolated from 110040 and transfected with scramble control, siHIF1α, or siHIF2α when cultured in 1% O_2 for 24 hrs. n=4. (P-Q) RNA-ChIP was used to detect the association of pri-let-7i with endogenous HIF1α (P) or p68 (Q) in GICs cultured in 1% O_2 for 24 hrs. HIF1α or p68 was immunoprecipitated separately in GICs isolated from 110040. Incorporation of pri-let-7i was examined by qPCR. IgG was used as a negative control. For HIF1α IP, n=4. For p68 IP, n=3. β-Actin or Histone H3 was used as an internal control for western blot. ACTB was used for the internal control of pri-miRNAs and mRNAs. RNU6 was used as an internal control for pre- and mature miRNAs. Data are represented as the mean ± SEM. (* $p<0.05$, ** $p<0.01$, *** $p<0.001$)

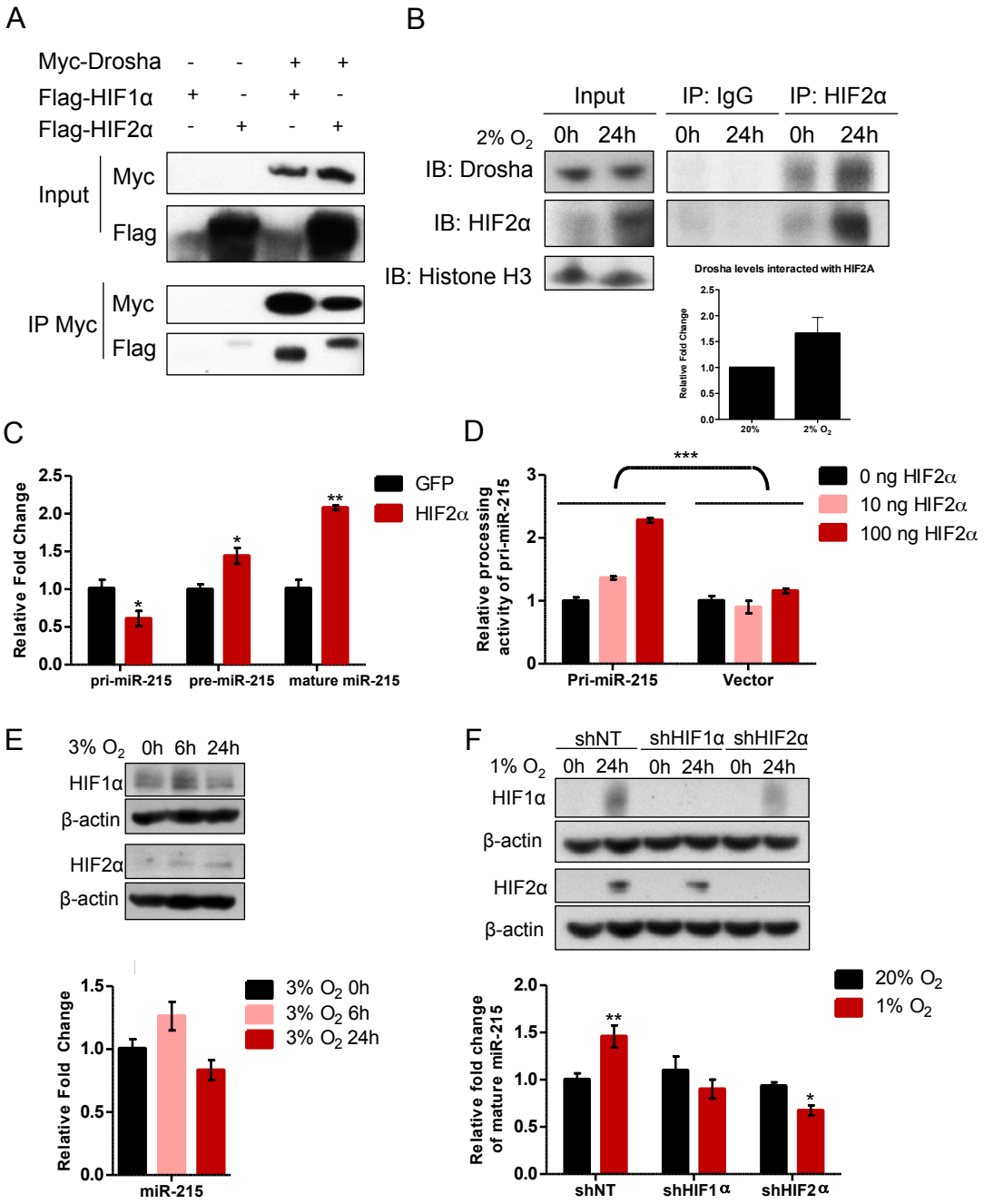

Figure S4, Related to Figure 3. HIF2α functions in a similar way as HIF1α to interact with Drosha and mediate processing of pri-miR-215. (A) Co-immunoprecipitation was used to detect the interaction between Myc-tagged Drosha and Flag-tagged HIF1α or Flag-tagged HIF2α when they were expressed in HEK293T cells. (B) Co-immunoprecipitation of endogenous HIF2α was performed in 110040 GICs cultured in 2% O_2 for 24 hrs followed by determination of protein level of the associated Drosha through Western blot. Quantification of Drosha levels interacted with HIF2α under hypoxia was shown in the lower panel, as measured by Image J. IgG was used as a negative control for IP. (C) Expression levels of pri-, pre- and mature miR-215 were detected by qPCR in HEK293T cells transfected with a stabilized HIF2α mutant or GFP control. (D) Processing activity of pri-miR-215 by Drosha *in vivo* was determined using a luciferase-pri-miR-215 reporter or control over-expressed in HEK293T cells. Different amounts of the stabilized HIF2α mutant were transfected. The processing activity was calculated by the luciferase activity normalized to the internal renilla luminescence from the same reporter plasmid. n=3. (E) Immunoblots

were performed to examine protein levels of HIF1α and HIF2α; qPCR was performed to measure expression level of miR-215 in D456MG CD133$^+$ GICs cultured under 3% O_2 for the indicated time points. n=4. (F) Immunoblots were performed to examine protein levels of HIF1α and HIF2α; qPCR was performed to measure expression level of miR-215 in D456MG CD133$^+$ GICs expressing shNT, shHIF1α or shHIF2α when cultured under 1% O_2 for 24 hrs. β-Actin or Histone H3 was used as an internal control for western blot. ACTB was used for the internal control of pri-miRNAs. RNU6 was used as an internal control for pre- and mature miRNAs. Data are represented as the mean ± SEM. (* p<0.05, **p<0.01)

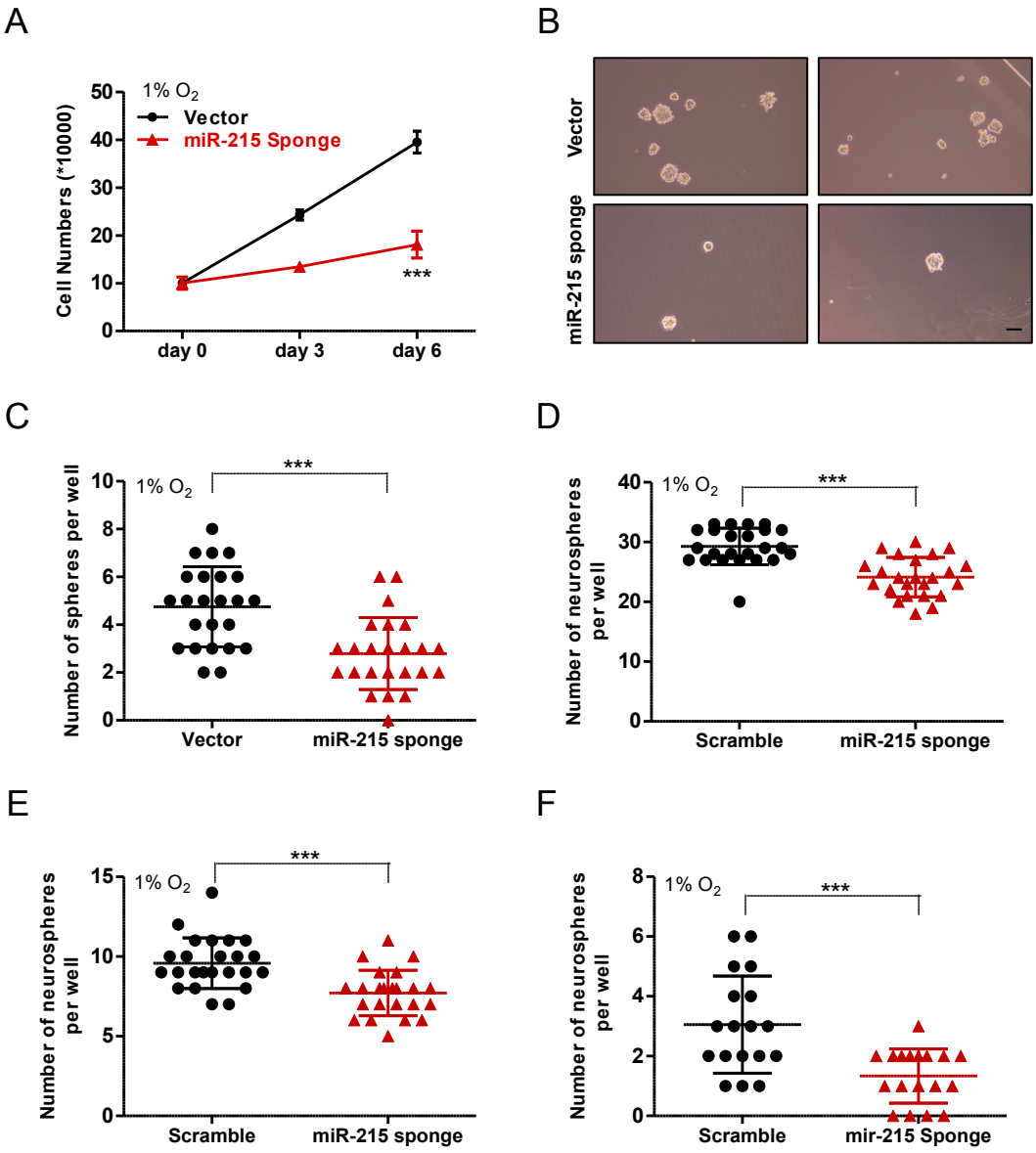

Figure S5, Related to Figure 4. Suppression of miR-215 attenuates the growth and neurosphere formation by GICs under hypoxia. (A) Cell numbers were counted for the CD133$^+$ D456MG GICs expressing a scramble control or miR-215 sponge when cultured under 1% O_2. n=4. (B) Representative pictures of neurospheres formed by D456MG GICs expressing vector control or miR-215 sponge. Scale bar: 50μm.(C-F) Neurosphere formation assay was performed in D456MG CD133$^+$ GICs (C), 080695 CD133$^+$ GICs (D), GSC20 (E), D456MG CD15$^+$ GICs (F) expressing indicated plasmids when cultured under 1% O_2. 50 cells were plated in each well of 24-well plates. Data are represented as the mean ± SEM. (* p<0.05, **p<0.01, ***p<0.001)

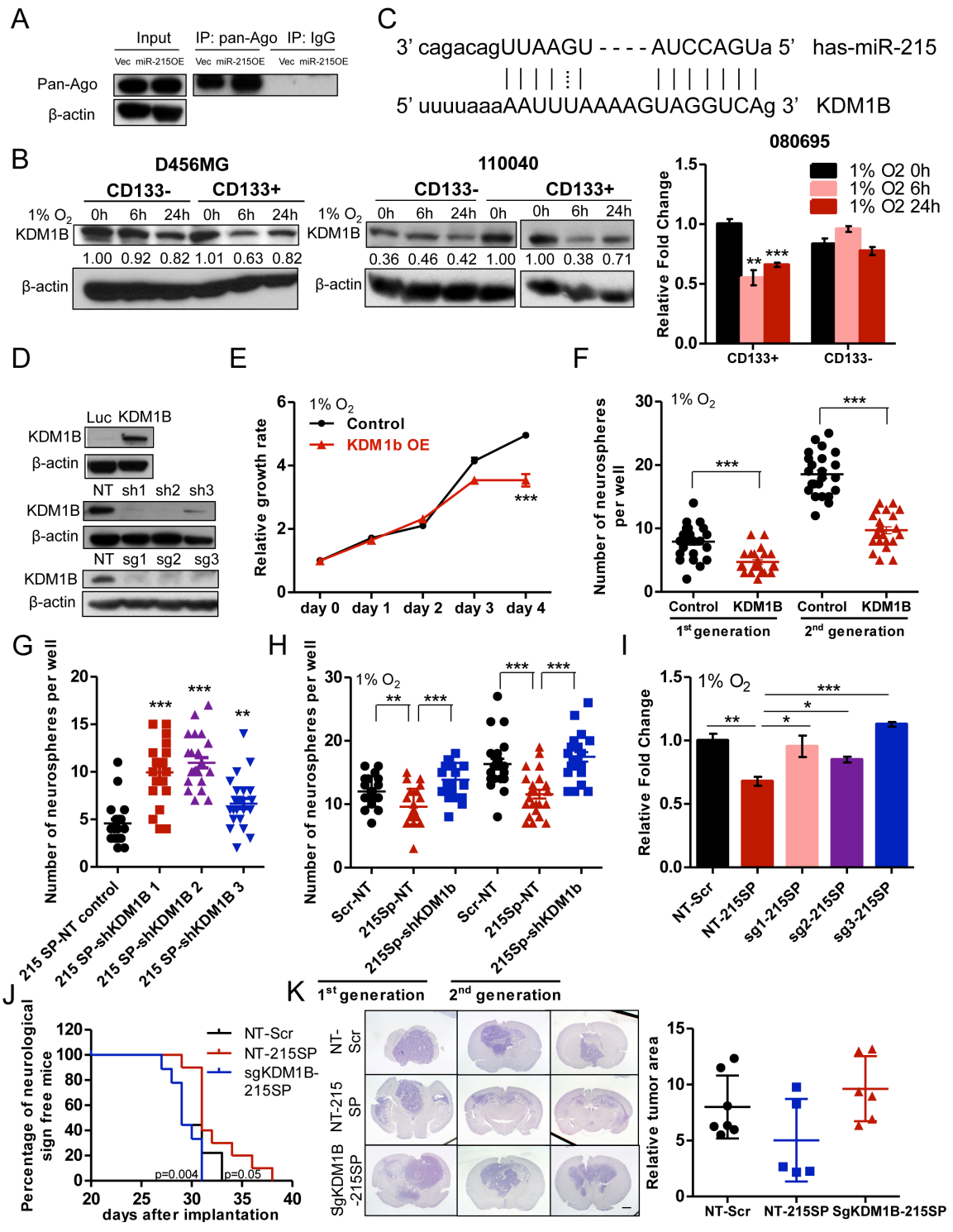

Figure S6, Related to Figure 5. Identification of KDM1B as a direct target mediating the function of miR-215 in maintaining the properties of GICs under hypoxia. (A) Immunoblots were used to detect the Ago2-RISC complex using the Ago antibody from D456 GICs with miR-215 overexpression or control. IgG was used as a negative control. (B) Protein and mRNA levels of KDM1B were measured by immunoblots and qPCR in paired CD133^{+} GICs and CD133^{-} non-GICs isolated from D456MG (protein

level), 110040 (protein level) and 080695 (mRNA level, n=3) when cultured under 1% O_2 for the indicated time points. (C) Alignment of miR-215 and its binding site in the 3'UTR of KDM1B. (D) Immunoblots were used to determine the protein level of KDM1B in $CD133^+$ D456MG GICs over-expressing the Luciferase control or the ORF of KDM1B (upper panel); non-targeting control or three shRNAs targeting different regions of KDM1B (middle panel); Cas9 and non-targeting control or three single-guide RNAs (sgRNA) targeting different regions of KDM1B (bottom panel). (E) Cell growth rate was measured by cell titer glo (Promega) in the D456MG GICs expressing the indicated plasmids. n=4. (F-H) Neurosphere formation assay was performed in D456MG GICs expressing the indicated plasmids. (I) Cell growth rate was measured by cell titer glo (Promega) in the D456MG GICs expressing the indicated plasmids. n=4. (J) Kaplan-Meier curves were drawn to measure the burden of tumor progression by D456MG GICs expressing the indicated plasmids. 5000 cells were implanted intracranially in each mouse. n=9. (K) H&E staining of brain sections showed intracranial tumors that were formed 29 days after implantation of 5000 $CD133^+$ D456MG GICs expressing the indicated plasmids. Pictures were taken at the maximum cross section of tumors from each brain. Tumor areas from H&E staining were quantified using ImageJ. n=5. Scale bar: 1.0 mm. For the neurosphere formation assay, 50 cells were plated in each well of 24-well plates. Data are represented as the mean ± SEM. β-Actin was used as an internal control for western blot. ACTB was used as an internal control for qPCR. (* $p<0.05$, ** $p<0.01$, *** $p<0.001$)

Tables S3, Related to Figure 5. MRNAs regulated by miR-215

Function of miR-215 was suppressed either by miR-215 LNA inhibitor or by miR-215 sponge in GICs isolated from 11-0040 and D456MG under hypoxia. In the meantime, GICs without gene manipulation were cultured under hypoxic and normoxic conditions. 14 genes were commonly up-regulated when miR-215 was blocked, and consistently down-regulated under hypoxia compared to normoxia conditions.

mRNA	11-0040 1% O_2 12h		D456MG 1% O_2 12h		1% O_2 / 20% O_2	
	LNA/NC	sponge/NC	LNA/NC	sponge/NC	11-0040	D456MG
KDM1B	1.60	3.65	1.43	1.90	0.44	0.45
HSDL2	1.31	1.36	1.41	1.48	0.36	0.37
FAM98A	1.20	2.17	1.35	1.41	0.82	0.49
SLC7A6	1.28	2.82	1.48	1.37	0.89	0.74
RAB2A	1.85	2.34	1.39	0.70	0.76	0.44
CTCF	1.36	2.19	1.32	1.29	1.01	0.70
MCM10	1.28	1.49	1.31	0.97	0.54	0.43
CPD	1.54	2.28	1.31	1.37	0.96	0.89
SEC62	1.20	2.63	1.19	1.45	0.94	0.86
CD164	1.46	1.81	1.21	1.05	1.07	0.79
DPY19L3	1.43	1.40	1.79	1.03	0.79	0.71
C1orf124	1.41	2.59	1.18	1.25	0.63	0.83
DBT	1.26	1.24	1.19	1.01	0.63	0.38
UPF2	1.19	2.04	1.17	1.24	0.67	0.68

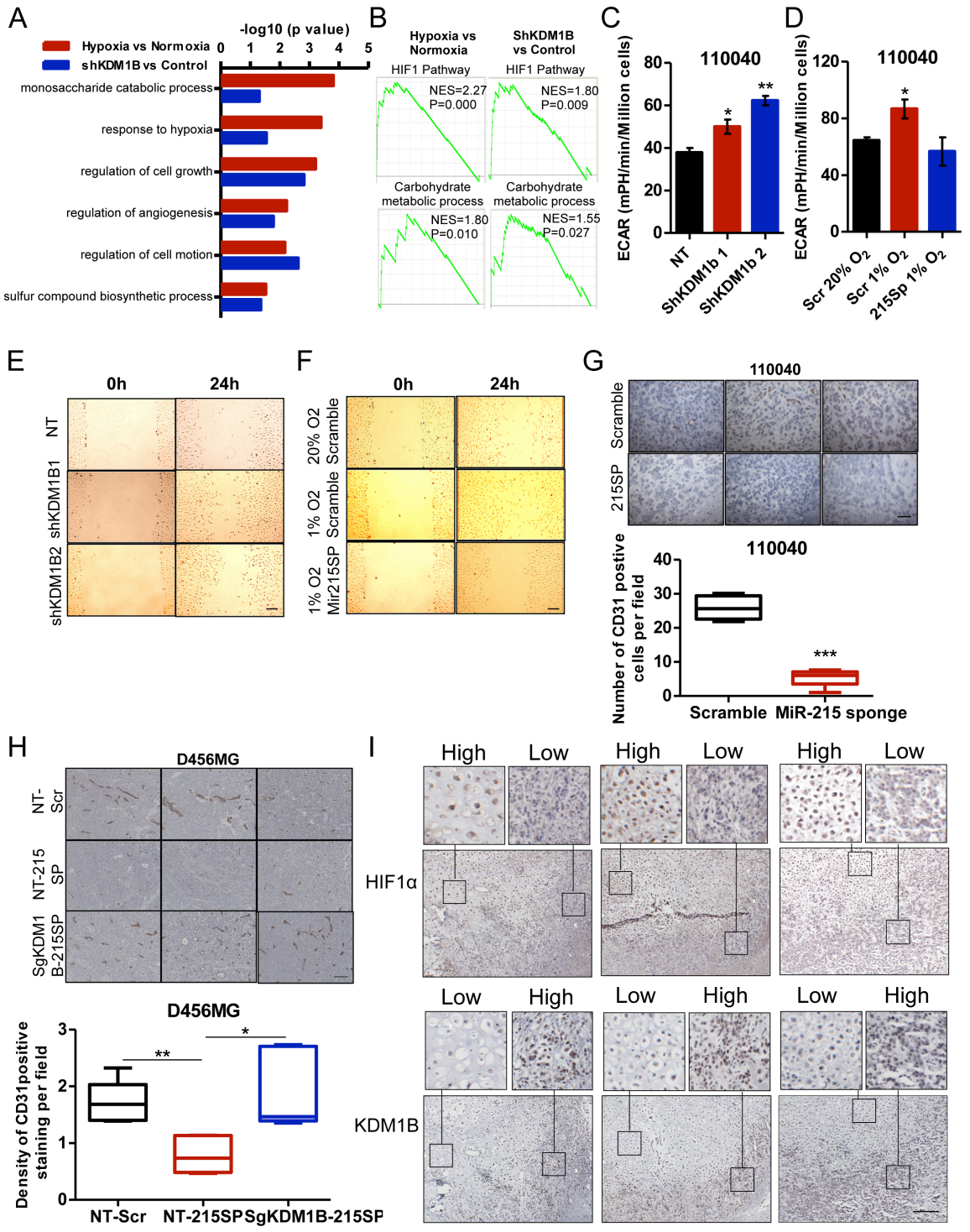

Figure S7, Related to Figure 6. KDM1B modulates activities of multiple pathways. (A) Gene ontology analysis was performed by DAVID BIOINFORMATICS to identify the enriched biological processes among the list of de-regulated genes in GICs with suppression of KDM1B and another list of altered genes in GICs cultured under hypoxia. The significantly enriched processes identified from those two gene lists were overlapped. (B) Significantly enriched processes and their p values as well as enrichment scores were analyzed by Gene Set Enrichment Analysis (GSEA, Broad Institute). (C, D) Extracellular Acidification Rate (ECAR) was measured from 110040 GICs with the indicated modifications and culturing conditions.

n=3. (E, F) Representative pictures showing the status of wound closure from immortalized human microvascular endothelial cells cultured in the conditional media harvested from 110040 GICs with the indicated modifications and culturing conditions. Scale bar: 50μm. (G) Representative pictures showing the CD31 staining of the intracranial tumors generated from 110040 GICs expressing scramble control or miR-215 sponge (Upper panel). Scale bar: 50μm. Bottom panel shows the quantification of CD31 positive cells from each field in the two groups. n=5. (H) Representative pictures showing the CD31 staining of the intracranial tumors generated from D456MG GICs expressing the indicated plasmids (upper panel). Scale bar: 100μm. Bottom panel shows the quantification of CD31 positive staining from each field measured by Image J. n=5. (I) Representative pictures showing the nuclear staining of HIF1α (upper panels) and KDM1B (bottom panels) in serial sections from 110040 xenografts. Scale bar: 200μm. Representative corresponding areas with HIF1α high (KDM1B low) or HIF1α low (KDM1B high) staining were shown in the enlarged pictures on top of each picture. Data are represented as the mean ± SEM. (* $p<0.05$, ** $p<0.01$, *** $p<0.001$)

Supplemental Experimental Procedures

MicroRNA profiling. MicroRNA profiling was conducted as described previously (Wang et al, 2014b). Total RNA from cells cultured under normoxia or hypoxia was extracted using the mirVana^{TM} miRNA Isolation Kit (Ambion) and reverse transcribed by the RT^2 miRNA First Strand Kit (Qiagen). Expression of miRNAs was examined by qPCR using RT^2 miRNA PCR Array (Qiagen), which contains 88 miRNAs with potential functions related with cell differentiation and development. Human RNU6 was measured as a control.

Microprocessor activity reporter assay. Sequence of pri-miR-215 (Forward primer: TGTGGTCACTTGGACTCTCATTTGA; Reverse primer: ATGGTACATAGGTTGACTGGTCAGT) was cloned into the 3'UTR of the firefly luciferase within the pmirGLO plasmid (Promega). For luciferase reporter assay, HEK293T cells were co-transfected with 1 ng luciferase constructs and 0ng, 10ng, 100ng HIF1α or HIF2α over-expressing plasmid respectively in 96-well plate. Firefly and Renilla luciferase activities were measured using the Dual-Luciferase Reporter Assay (Promega) 48 hrs after transfection. The processing activity was calculated by the luciferase activity normalized to the internal renilla luminescence from the same reporter plasmid.

Northern blot assay. According to the previous report (Pall and Hamilton, 2008), 30 μg RNA from HEK293T cells transfected with pri-miR-215 and a stabilized HIF1α or GFP control was separated in a 15% denaturing acrylamide gel (Invitrogen) and transferred onto Hybond NX membrane (GE Healthcare Life Sciences). Cross-linking was performed using 1-ethyl-3-(3-dimethylaminopropyl) carbodiimide (EDC) (Sigma) -mediated method. LNA miR-215 and U6 probes (Exiqon), as well as RNA ladder (Decade Marker System from Invitrogen) were labeled at the 5' end with radioactive P^{32} using T4 PNK (New England Biolabs) and subsequently cleaned with Microspin G-25 column (GE Healthcare Life Sciences). After crosslinking, the blot was pre-hybridized using ULTRAhyb (Invitrogen) for 1 hour and then incubated with radioactive probe overnight at 37 ^{0}C in a hybridization oven. Membrane was washed with Low Stringency Wash Solution 1 (Invitrogen) and exposed to X-ray film.

Plasmids, shRNAs and CRISPR/Cas9 system. MiR-215 sponge containing ten repeats of anti-sense miR-215 (GTCTGTCAAAGTTAGGTCAT), or a scramble sequence (AAGTTTTCAGAAAGCT AACA, (Ebert et al., 2007) was synthesized by GenScript and cloned into pWPXLD vector (Addgene). Primary miR-215 was cloned into pWPXLD to overexpress miR-215. ShRNA clones (Sigma Mission RNAi) targeting KDM1B and scramble (SHC002) were purchased from Sigma. To generate CRISPR/Cas9 plasmid targeting KDM1B, primers of single-guide RNAs were annealed, ligated into LentiCRISPRv2 (Addgene) and transduced to GICs by lentivirus. KDM1B ORF (Forward primer: ATGGCAACTCCACGGGGG AG; Reverse primer: TTAAAATGCTG CAATCTTGCTTG) was amplified from human cDNA libraries and cloned into a Tet-on 3G plasmid modified from the backbone of pCDH-CMV-MCS-PURO (System Biosciences). GICs were cultured with doxycycline (1ug/ml) for 4 days to induce expression of KDM1B or Luciferase as a control. Virus was produced from HEK293T cells co-transfected with the packaging plasmids psPAX2, pCI-VSVG (Addgene) and the expression vectors described above by Lipofectamine 2000 (Invitrogen). The viral-infected GICs were selected by GFP or

puromycin (1ug/ml). To express stable Flag-tagged HIF1α or HIF2α under normoxia condition, HIF1α or HIF2α was amplified from HA-HIF1alpha P402A/P564A-pcDNA3 or HA-HIF2alpha-P405A/P531A-pcDNA3 (Addgene) separately with deletion of their stop codons into pcDNA3.1/Hygro(+) (Invitrogen). Two Flag-tags were then cloned into the C-terminal of these genes. To express Flag-Myc-tagged Drosha, Myc-Drosha was amplified from pcDNA4/TO/cmycDrosha (addgene) and cloned into p3xFlag-CMV10 (Sigma). These plasmids were transfected into HEK293T cells to express the specific proteins and cells were harvested 48 hours later.

Sequence of shRNA constructs

Name of constructs	TRC number	Clone ID	Sequence
sh-KDM1B	TRCN0000236734	NM_153042.3-1273s21c1	CCGGTCCCGGGTACTCGGTGATAATCTCGAGATTATCACCGAGTACCCGGGATTTTTG
sh-KDM1B	TRCN0000257375	NM_153042.3-3120s21c1	CCGGGGGTCTTCAGGATGCCTATTTCTCGAGAAATAGGCATCCTGAAGACCCTTTTTG
sh-KDM1B	TRCN0000236737	NM_153042.3-1173s21c1	CCGGTTAACAACCCAGTAGCATTAACTCGAGTTAATGCTACTGGGTTGTTAATTTTTG

Primer sequence of single-guide RNAs (sgRNA)

Gene	Forward Primer	Reverse Primer
sg-KDM1B1	CACCGCTCCGGATAGCCTTCCTTTG	AAACCAAAGGAAGGCTATCCGGAGC
sg-KDM1B2	CACCGTTGAGGAGCTCCGGTAGGCA	AAACTGCCTACCGGAGCTCCTCAAC
Sg-KDM1B3	CACCGAGCCTTCCTTTGAGGAGCTC	AAACGAGCTCCTCAAAGGAAGGCTC
NT control	ACGGAGGCTAAGCGTCGCAA	TTGCGACGCTTAGCCTCCGT

Primer sequences of the sgRNAs were from the previous study (Wang et al., 2014b).

LNA inhibitor and siRNA assays. LNA miR-215 inhibitor (TCTGTCAATTCATAGGT C) and a LNA scramble control (ACGTCTATACGCCCA) were synthesized by Exiqon. SiRNAs of HIF1α and HIF2α were synthesized by Invitrogen. 50pmole/ml LNA miR-215 inhibitor or 10pmole/ml siRNA was transfected into GICs using Lipofectamine RNAiMAX Reagent (Invitrogen). Experiments were performed 48 hours after transfection.

Primer sequences for siRNAs

siRNA	Forward primer	Reverse primer
HIF1α	CCAGCCGCUGGAGACACAAUCAUAU	AUAUGAUUGUGUCUCCAGCGGCUGG

HIF2α	CACCGGCCCAUGUCCUCCAUCUUCU	AGAAGAUGGAGGACAUGGGCCGGUG

RNA-ChIP and qPCR

RNA-ChIP was performed as described previously (Berkovich et al., 2008). All buffers used in the assay contained proteinase inhibitor (Sigma, P2714) and 0.3 U/μl SUPERase•In™ RNase Inhibitor (Life Technologies). 110040 or D456MG GICs cultured under hypoxia or normoxia for 24 hours were fixed with 1% formaldehyde, followed by nuclei isolation and chromatin fragmentation. Lysates were incubated with Dynabeads Protein G (Invitrogen) and anti- HIF1α (Novus, NB100-134), anti- HIF2α (Novus, NB100-122), anti-Drosha (Abcam, ab12286), anti-DDX5 (Abcam, ab21696), or IgG control (Jackson ImmunoResearch) antibodies respectively for immunoprecipitation. The beads were washed, then RNA was eluted, reverse-crosslinked and precipitated by ethanol with glycogen. After DNase I treatment and removal, one fourth of the RNA was used for reverse transcription and qPCR analysis to examine levels of the pri-miRNAs. Levels of the immunoprecipitated pri-miRNAs were normalized to their levels in the inputs.

To isolated RNA from RISC, experiments were conducted as described (Wang et al, 2014b), 110040 GICs with miR-215 overexpression or vector control were fixed with 1% formaldehyde, followed by chromatin fragmentation. Cells were lysed in PXL buffer and incubated with Dynabeads Protein A (Invitrogen) together with anti-pan Ago, clone 2A8 antibody (Millipore) or IgG control for immunoprecipitation. One forth of the immunoprecipitated RNA was reverse transcribed using iScript cDNA synthesis kit (Bio-Rad), followed by qPCR analysis.

Neurosphere formation assay. GICs with indicated modification or treatment were plated in 24-well plates with 50 cells per well by flow cytometry. After 7-10 days, the number of neuropspheres in each well was quantified. Spheres were dissociated to single cells and plated again in 24-well plates to form 2nd generation of neurospheres.

Immunoprecipitation and immunoblot assays

Immunoprecipitation was performed as described previously (Wang et al., 2014a). Nuclei were isolated from GICs cultured under hypoxia or normoxia for 24h, then lysed in NETN buffer (50 mM Tris, 150 mM NaCl , 1mM EDTA, 1% NP40, 10% glycerol, 1 mM Na3SO4 and 10 mM NaF) supplemented with protease inhibitors. The lysate was pre-cleared and incubated with anti-HIF1α, anti-HIF2α, or IgG control separately and Dynabeads protein G overnight at 4°C. Immunoprecipitates were washed four times in NETN buffer, boiled in SDS buffer and the supernatants were used for Western blot analysis. Similarly, cell lysates from HEK293T cells over-expressing the indicated plasmids were incubated with anti-cmyc (9E10, Zymed), anti-Flag (M2, Sigma) or IgG control for immunocprecipitation.

For immunoblot assay, cells were lysed in RIPA buffer (Sigma) containing protease inhibitors. Protein concentrations were determined with the BCA Protein Assay (Pierce). Quantified lysates were loaded on Novex SDS-PAGE (Invitrogen), transferred onto PVDF membrane (Millipore) and probed with rabbit anti-human HIF1 α (1:1000, Novus), HIF2α (1:1000; Novus), Drosha (1:1000; Abcam), DDX5 (1:1000; Abcam), KDM1B (1:1000; Abcam), and mouse anti-human β-actin (1:10000; Sigma), DGCR8 (1:1000; Abcam), P-smad 2/3 (1:1000; Santa Cruz), P53 (1:1000; Santa Cruz), mouse anti-Flag (1:5000; Sigma), mouse anti-cmyc (1: 500, Zymed) followed by incubation with secondary HRP-conjugated antibodies (1:5000; Invitrogen).

β-actin, γ-tubulin or Histone H3 was used as the internal control for immunoblot and immunoprecipitation assays as indicated.

Cell viability assay. As described previously (Wang et al, 2014b), GICs with indicated modifications or treatments were plated in 96-well plates (Costar) at 1500 cells per well. Plates were examined at the indicated time points by Cell Titer-Glo® Luminescent Cell Viability Assay kit (Promega).

Luciferase reporter assay. 3'UTR of KDM1B (Forward primer: TTCCATAGGCAGGTCCACT; Reverse primer: CTGTTGGCTTGTTTTGGGAC) containing the predicted binding sites of miR-215 was cloned into the pmirGLO luciferase reporter plasmid (Promega). The predicted binding sites were mutated from TAGGTCA to CGAACTG by PCR to generate the mutant 3'UTR. HEK293T cells were co-transfected with 1ng luciferase constructs and 0ng, 5ng, 10ng pri-miR-215 over-expressing plasmid respectively in 96-well plate. Firefly and Renilla luciferase activities were measured using the Dual-Luciferase Reporter Assay (Promega) 48 hours after transfection and the results were normalized as relative luciferase activity (Firefly luciferase/Renilla luciferase).

Cell scratch assay. Immortalized human microvascular endothelial cells were cultured with EBM-2 (Lonza) and EGM-2 MV SingleQuots (Lonza) in 6 well plates. Once the cell confluence reached to 100%, a scratch was made using the tip of P1000 pipette. Cells were washed with PBS and subsequently cultured under conditional media harvested from 110040 GICs with indicated modifications. Pictures were taken on three random areas of the wound for each group at the start point and 24 hours later. There were three wells (n=3) for each group. The percentage of wound closure rate was used to measure the migratory ability.

Glucose uptake assay. Glucose uptake was performed as described in literature (Liu et al., 2014). Briefly, 110040 GICs were washed once in PBS and re-suspended in KRH (Krebs-Ringer-HEPES) buffer with 0.2 million cells/reaction. 2-deoxy-D-^{3}H glucose (2uCi/reaction) was added into each reaction and cells were incubated for 10 minutes at 37°C. 200uM of ice-cold phloretin (Calbiochem, Gibbstown, NJ) was injected at the end of incubation. Cells were pelleted through an oil layer (1:1 mix of Dow Corning 550 Silicon fluid, Motion Industries, Brimingham, AL; and dinonyl phthalate from Sigma-Aldrich). Remaining 2-deoxy-D-^{3}H glucose was removed. Cell pellets were lysed using 1M NaOH and radioactivity was measured with a scintillation counter. Data was normalized to the cell number in each reaction.

Extracellular acidification rate (ECAR) assay. ECAR was measured using a 24-well XF extracellular flux analyzer as described before (Liu et al., 2014). Briefly, 0.15 million 110040 GICs were seeded in each well and incubated in a non-CO_2 incubator for one hour in XF media supplemented with 2mM glutamine and 25mM glucose prior to starting the assay. Six repeated measurements were taken for baseline ECAR. Following the six measurements, 2-DG was injected into each well at a final concentration of 20mM. Three replicate wells were set up for each group. Measurements of ECAR were normalized to cell number.

Chondroitinase ABC treatment. GICs were dissociated to single cells and cultured in the media with Chondroitinase ABC (0.05U/ml, Sigma) or control for the indicated time, followed by the cell viability and neurosphere formation assays.

Intracranial tumor assays. GICs with the indicated numbers were implanted into the left or right frontal lobes of athymic BALB/c nu/nu mice under a protocol approved by Duke University Institutional Animal Care and Use Committee. Mice were maintained until the development of neurologic symptoms. Specific neurological signs mainly include hunched back, head tilt and loss of balance. There is also moderate stress such as loss of body weight, eat less and inactivity (Kramp and Camphausen, 2012). Brains of euthanized mice were collected, fixed in 4% PFA, paraffin embedded, and sectioned for H&E and IHC staining.

ISH and IHC staining in GBM tissue microarrays. As illustrated previously (Wang et al, 2014b), the same tissue microarray with a total of 107 paraffin-embedded glioblastoma tissues was used for analysis, which had been clinically and histopathologically diagnosed at the Department of Neurosurgery, the Second and Fourth Affiliated Hospitals of Harbin Medical University in China, from 2002 and 2007. The histological features of all the specimens were confirmed by pathologists according to the WHO criteria and listed in the literature (Wang et al, 2014b). In situ hybridization was used to examine the expression of miR-215 using a Cy3-labelled miR-215 probe (RiboBio). The signals of in situ hybridization of tissue sections were examined and scored separately by two independent investigators blinded to the histopathological features and patient data of the samples. MiR-215 expression was evaluated according to the proportion of positively stained tumor cells and the intensity of staining. The proportion of positively stained tumor cells was graded as follows: 0, no positive tumor cells; 1, 0.01–25% positive tumor cells; 2, 25.01–50% positive tumor cells; 3, 50.01–75% positive tumor cells; 4, $\geq$ 75% positive tumor cells. The cells at each intensity of staining were recorded on a scale of 0 (no signal), 1 (weak), 2 (moderate), and 3 (strong). The hybridization score for each section was computed by the following formula: hybridization

score = staining intensity × proportion of positively stained tumor cells. A total score of 0–12 was calculated and graded as negative (-, score: 0), weak (+, score: 1–4), moderate (++, score: 5–8) or strong (+++, score: 9–12). Cutoff values to define the high- and low-expression of miR-215 were chosen on the basis of a measurement of heterogeneity with the log-rank test statistic with respect to overall survival. Because the optimal cutoff threshold were identified from the current study as 5, an hybridization score ≥ 5 was taken to define tumors as high expression, and hybridization score < 5 to define tumors as low expression of miR-215. The quantification of immunohistochemical staining of KDM1B and HIF1α was performed in the same manner as for miR-215. KDM1B antibody was purchased from LifeSpan Biosciences, Inc., HIF1α antibody was from Novus and IHC was carried out according to the instruction by the company.

H&E and IHC staining. Paraffin embedded tumor-bearing brains from 110040 or D456MG GICs expressing the indicated plasmids were serially sectioned at 5μm in thickness using microtome (Leica). To evaluate tumor growth, the whole brain was sectioned from most anterior to posterior. H&E staining was further performed in all the locations of each brain to determine the locations from beginning to the end of each tumor. After careful comparison, the section with the biggest tumor area for each brain was used for the measurement. Briefly, sections were deparaffinized with xylenes (Fisher Scientific), incubated with a series of concentration gradient of ethanol, followed by treatment with Harris Hematoxylin (Leica) for 2.5 minutes. After wash, sections were incubated with PROTOCOL Bluing Agent (Fisher Scientific) for one minute and acidic eosin for two minutes. For CD31 staining, sections were dehydrated and incubated with peroxide block (Sigma) for 15 minutes, followed by antigen-retrieval in the citrate buffer (pH 6.0) for 10 minutes at 110°C using a pressure cooker. Sections were then blocked and probed with rabbit anti-human PECAM-1 (1:3000, Santa cruz) at 4°C overnight. After wash, sections were incubated with secondary HRP-conjugated antibody (DAKO) and developed with DAB development substrate (DAKO). Sections from two different locations of each tumor-bearing brain were stained. At least three random pictures were taken for each section. Some tumors generated by the miR-215 sponge were not big enough, thus one or two pictures were taken to capture the random areas for those sections. CD31 positive cells were counted in all the pictures and quantified.

MRNA and small RNA sequencing. MRNA sequencing was performed as described previously (Ouyang et al., 2014; Zhou et al., 2014). Briefly, D456MG GICs expressing non-targeting control or shKDM1B were harvested. Total RNA was extracted by RNeasy mini Kit (Qiagen) and treated with DNase I on column, according to the manufacture's instructions. 2ug RNAs were firstly reverse transcribed to cDNA using Superscript III Reverse Transcriptase (Invitrogen) with primer Biotin-B-T. The cDNA was purified by NucleoSpin Gel and PCR Clean-Up Kit (Clontech) to remove free RT primers and enzyme. Terminal transferase (NEB) was further employed to block the 3' end of the cDNA. The cDNA was then isolated by the streptavidin-coated magnetic beads (Life Technology). After that, second-strand cDNA was synthesized by random priming with primer A-N8, eluted and amplified by PCR to construct libraries with barcode primers and primer PB. Finally sequencing was performed with P5 primer on Hiseq 2000 system and sequencing reads were mapped to hg18 from UCSC genome browser. For small RNA sequencing, 110040 GICs collected at different time points in 1% O_2 or 20% O_2 were lyzed in Trizol (Life Technology). Total RNA was then extracted, digested with RQ1 DNase, and analyzed using bioanalyzer (Agilent). For each small RNA library, 10 μg of total RNA was subjected to the small RNA library preparation kit (Illumina) using the alternative v1.5 protocol with some modifications. After ligated with 3' and 5' RNA adapters, RNA samples were reverse transcribed using diluted SRA RT primer and PCR amplified for 10 cycles using multiplex primers. The PCR products were then separated from 15% Novex TBE gel (Life Technology). DNA at sizes between 90-100 bp was resolved from the gel and quantified using Qubit fluorometer (Life Technology). Afterwards, 2ng of each sample was mixed together for sequencing using P5 primer (GTTCAGAGTTCTACAGTCCGACGATC). After sequencing, the sequence tags were mapped to the sequences that correspond to intended ligation products and segregated for individual samples based on their barcodes. The sequences were then mapped to miRBASE database. For analysis, sequencing tags lower than 100 reads were cut off and the rest were normalized according to the total reads of each sample and compared. There are three biological replicates for each experimental group in the small RNA and mRNA sequencing.

QRT-PCR for measuring mRNA expression. Total RNA was extracted using the RNeasy mini Kit (Qiagen), then reverse transcribed into cDNA using iScript cDNA synthesis kit (BioRad). MRNA levels were measured using SYBR Green mix (Quanta) and a Mastercycler® Realplex system (Eppendorf). ACTB or RPLP0 was used as an internal control.

Primer sequences of mRNA for qPCR

Gene	Forward Primer	Reverse Primer
ACTB	CATCCACGAAACTACCTTCAACTCC	GAGCCGCCGATCCACACG
RPLP0	ATCTGCTTGGAGCCCACAT	GCGACCTGGAAGTCCAACTA
KDM1B	GGAACCGTCTTTTTCGCTGG	TTCCCCATCTGGGGTACAGA
HSDL2	CAGGCAGATGTGGTGATGAGT	TGCTAGGGCCATGTTACCTT
FAM98A	GGAGTGTGACCTCATGGAGAC	AGAGCGCTCCATCTTCCAAC
SLC7A6	CCCACTTGACATAGGCACAG	CTACATCATCCAGCCGTCCT
RAB2A	ATTGGTGTAGAGTTCGGTGCTC	ACCAGGTTGTCAAGTGGTTG
CTCF	TAATTGTGCTGGCCCAGATG	TCATCCTCATTGTCGTCCAGA
MCM10	GCGGTCAGCAGAGACAGATT	CGGCCAAGATTCTACATTGC
CPD	AAACAGTTGGCCCACACATA	TGTCCAGGAGATGAAGACGA
SEC62	TTGGTGGACTTTGTTGGACA	GAACGCAGGAGACACAAGAA
CD164	CAAGTGGGGAACACGACAGA	GCTGTAGAATTGGCTGTTGGC
DPY19L3	CAGGCCACACTCTGTTCTGA	ACATCTGTCTACCTTGCCACG
C1orf124	CCTTCTCGGTCTTTGTCGTT	AGCGAACCCCTTTTGAAGTT
DBT	TTTCGGCCCTTTATCTCTTG	CCTATGTGGGGAAGCCATTA
UPF2	CCCTCAGCATGGAACAAAGA	TTGGTACGGGCACTCTTCAT
TYMS	GCAGTTGGTCAACTCCCTGT	AGAGAAGAAGGGGACTTGGG
PTPRT	CCACAGTTGCTGTAGTGCTCA	GCCTGCTCCTGAGGCTG
RB1	TCAGTTGGTCCTTCTCGGTC	TGTGAACATCGAATCATGGAA
CTNNBIP1	AGCTACTGCCTCCGGTCTTC	GTGGTCAACAGCCAGCTCA
ACVR2B	AGGCCGCTCTGGTTGGT	CCCTCCTCTGGGGATCG
NDUFA4L2	TCCGGGTTGTTCTTTCTGTC	CGATGATCGGCTTAATCTGC
SLC2A1	GGCATTGATGACTCCAGTGTT	ATGGAGCCCAGCAGCAA
SLC2A3	GATGGGCTCTTGAACACCTG	GACAGCCCATCATCATTTCC
SERPINE1	ACCGCAACGTGGTTTTCTCA	TTGAATCCCATAGCTGCTTGAAT
HIF1A	TCCATGTGACCATGAGGAAA	CCAAGCAGGTCATAGGTGGT
EPAS1	CCCCACAGTGCTACGCCACC	GCACGGGCACGTTCACCTCA
NDRG1	GCCGCCTCCAAGATCTCA	ACGTTACTCTGCATTTCTTCCTTC
VEGFA	TGCTGTCTTGGGTGCATTGG	GCATAATCTGCATGGTGATGTTGG
ADM	ACGGAAACCAGCTTCATCC	GCCAGTGGGACGTCTGAG
LAMA5	GGCAAACTTGATGAGGACGTA	GCTGGTGGCAGAGTCCAC
CHST11	GCAGGACAGCAGTGTTTGAG	TCCCTTTGGTGTGGACATCT
CHPF	CAGCAGCCTCTGCCTGAT	GTCTTGCCCTACCACCCTG
DICER	GTACGACTACCACAAGTACTTC	ATAGTACACCTGCCAGACTGT

Primer sequences of pri- and pre-miRNA for qPCR

miRNA	Forward Primer	Reverse Primer
pre-miR-215	ATGACCTATGAATTGACAGACAAT	TTGGCCTAAAGAAATGACAGAC
pri-miR-215	AGTTTTGTAACACCAAAAAGATCCA	TTGGCCTAAAGAAATGACAGAC
pre-miR-126	TATTACTTTTGGTACGCGCTG	GCGCATTATTACTCACGGTAC
pri-miR-126	TGCCCGGAGCCTCATATCA	GCGCATTATTACTCACGGTAC

pre-miR-21	TGTCGGGTAGCTTATCAGAC	TGTCAGACAGCCCATCGACT
pri-miR-21	TTTTGTTTTGCTTGGGAGGA	AGCAGACAGTCAGGCAGGAT
pre-let-7i	TGTGCTGTTGGTCGGGT	GCAGTAGCTTGCGCAGTT
pri-let-7i	AGGAAGGACGGAGGAGC	GCAGTAGCTTGCGCAGTT
pre-miR-140	CAGTGGTTTTACCCTATGGTAGG	CGTGGTTCTACCCTGTGGTAG
pri-miR-140	TTTTCCGTGGTGACCTCCTC	CGTGGTTCTACCCTGTGGTAG
pre-miR-654	AAAGATGGTGGGCCGCAGAA	GGGCTTCTAAAGGTGATGGTCAG
pri-miR-654	GGGATCATGGCTGGACTGAAG	GGGCTTCTAAAGGTGATGGTCAG
pre-miR-210	CCTGCCCACCGCACACT	AGCCGCTGTCACACGCA
pri-miR-210	GCCCCTCAGAGGCCG	AGTGTGCGGTGGGCA
pre-miR-1260a	CTTTCCAGCTCATCCCACC	TTTTTGGCACTCCCTCTGAC
pri-miR-1260a	CTCACCTGAAGAAGCAGGAC	TTTTTGGCACTCCCTCTGAC

Supplemental References

Berkovich, E., Monnat, R.J., and Kastan, M.B. (2008). Assessment of protein dynamics and DNA repair following generation of DNA double-strand breaks at defined genomic sites. Nat Protoc *3*, 915-922.

Ebert, M.S., Neilson, J.R., and Sharp, P.A. (2007). MicroRNA sponges: competitive inhibitors of small RNAs in mammalian cells. Nat Methods *4*, 721-726.

Kramp, T.R., and Camphausen, K. (2012). Combination radiotherapy in an orthotopic mouse brain tumor model. Journal of visualized experiments : JoVE, e3397.

Liu, T., Kishton, R.J., Macintyre, A.N., Gerriets, V.A., Xiang, H., Liu, X., Abel, E.D., Rizzieri, D., Locasale, J.W., and Rathmell, J.C. (2014). Glucose transporter 1-mediated glucose uptake is limiting for B-cell acute lymphoblastic leukemia anabolic metabolism and resistance to apoptosis. Cell death & disease *5*, e1470.

Ouyang, H., Xue, Y., Lin, Y., Zhang, X., Xi, L., Patel, S., Cai, H., Luo, J., Zhang, M., Zhang, M.*, et al.* (2014). WNT7A and PAX6 define corneal epithelium homeostasis and pathogenesis. Nature *511*, 358-361.

Pall, G.S., and Hamilton, A.J. (2008). Improved northern blot method for enhanced detection of small RNA. Nat Protoc *3*, 1077-1084.

Wang, Q., Goldstein, M., Alexander, P., Wakeman, T.P., Sun, T., Feng, J., Lou, Z., Kastan, M.B., and Wang, X.F. (2014a). Rad17 recruits the MRE11-RAD50-NBS1 complex to regulate the cellular response to DNA double-strand breaks. The EMBO journal *33*, 862-877.

Wang, T., Wei, J.J., Sabatini, D.M., and Lander, E.S. (2014b). Genetic screens in human cells using the CRISPR-Cas9 system. Science *343*, 80-84.

Zhou, Y., Li, H.R., Huang, J., Jin, G., and Fu, X.D. (2014). Multiplex analysis of polyA-linked sequences (MAPS): an RNA-seq strategy to profile poly(A+) RNA. Methods in molecular biology *1125*, 169-178.